Order−Disorder Transitions and Magnetic Behaviour in Lithium Ferrites $Li_{0.5+0.5x}Fe_{2.5-1.5x}Ti_xO_4$ (x = 1.28 and 1.50)

María Ángeles Arillo,[a] María Luisa López,[a] Carlos Pico,[a] María Luisa Veiga,*[a] Javier Campo,[b] José Luis Martínez,[c] and Alejandro Santrich-Badal[c]

Keywords: Lithium ferrites / Order−disorder phenomena / Spinels / Spin-glass behaviour

We report the structural characterization and magnetic behaviour of the spinels with general formula $Li_{0.5+0.5x}Fe_{2.5-1.5x}Ti_xO_4$, where x = 1.28 and 1.50. When the samples are cooled slowly, a 1:3 crystallographic order occurs, whereas a random disorder is observed when the samples are quenched. Neutron-powder-diffraction measurements were performed on the materials to characterize the structural transitions. Magnetic properties were studied by magnetic susceptibility (dc and ac), magnetisation and neutron-diffraction data and the results can be interpreted on the basis of a spin-glass behaviour.

Introduction

Lithium iron spinels, usually known as lithium ferrites, have been thoroughly studied materials because they are remarkably useful in many branches of technology.[1] The lithium ferrite $Li_{0.5}Fe_{2.5}O_4$ is known to occur in two crystalline forms.[2] Below 1008 K, there exists a 1:3 ordering of Li^+ and Fe^{3+} ions along the [110] directions of the unit cell, giving rise to the structural formula $(Fe)_T(Li_{0.5}Fe_{1.5})_OO_4$, in such a way that each lithium ion is followed by three iron cations that are all in octahedral coordination with oxygen ions. The remaining iron ions are located on the tetrahedral sites (space group $P4_332$).[3] Above 1000−1030 K, the 1:3 ordering is destroyed and the two types of cations are randomly distributed over the octahedral sites; the resulting phase is referred to as the disordered phase (space group $Fd3m$). By quenching rapidly from a high temperature, this latter phase can be retained indefinitely at room temperature or below.[4] The disordered $Li_{0.5}Fe_{2.5}O_4$ has an inverse spinel structure, with Fe^{3+} ions at tetrahedral 8*a* positions and Li^+ and Fe^{3+} ions distributed randomly over the 16*d* octahedral sites. The order−disorder transition in the lithium ferrite structure has been recorded by X-ray powder diffraction, and the relationship between the Wyckoff's positions of the $Fd3m$ and $P4_332$ states are as follows[5]:

$Fd3m \rightarrow P4_332$

$8a\ (8\ Fe^{3+}) \rightarrow 8c\ (8\ Fe^{3+})$

$16d\ (12\ Fe^{3+} + 4\ Li^+) \rightarrow 12d\ (12\ Fe^{3+}) + 4b\ (4Li^+)$

$32e\ (32\ O^{2-}) \rightarrow 24e\ (24\ O^{2-}) + 8c\ (8\ O^{2-})$

The magnetic properties of a spinel ferrite depend on their structural features, both of which are quite sensitive to the preparation conditions as well as to the amount and type of substitution. The most synthetically advantageous characteristic of spinel materials is that various ions can be placed at tetrahedral and octahedral sites within the structure, a situation that allows for control of their magnetic properties. In addition to ferromagnetism and antiferromagnetism (ferrimagnetism), another unique spin state − the so-called spin-glass (SG) state − can be assigned to spinel ferrites. The substitution of iron atoms by tetravalent titanium influences the above properties. Solid solutions of general formula $Li_{0.5+0.5x}Fe_{2.5-1.5x}Ti_xO_4$ ($0 \le x \le 1.67$) crystallise in the space groups $P4_332$ (in the ranges $0 \le x \le 0.4$ and $1.2 \le x \le 1.57$) and $Fd3m$ (in the ranges $0.4 \le x \le 1.2$ and $1.57 \le x \le 1.67$).[5,6] Several authors[6−9] have reported detailed studies using X-ray diffraction and Mössbauer spectroscopy for the structural resolution of this system in the range $1.1 \le x \le 1.67$, in agreement with the cation distribution proposed by Blasse[5] and White[10]. On the other hand, Dormann's group has proposed that this system shows local canted spin behaviour (LCS).[11−14] With increasing dilution of Fe atoms, the distribution of the canting angles enlarges and the average canting angle

[a] Departamento de Química Inorgánica I, Facultad de Ciencias Químicas, Universidad Complutense,
28040 Madrid, Spain
Fax: (internat.) +34-91-3944352
E-mail: mlveiga@quim.ucm.es
[b] Institut Max von Laue − Paul Langevin (ILL),
38042 Grenoble Cedex 9, France
[c] Instituto Ciencia de Materiales de Madrid, CSIC, Cantoblanco,
28049 Madrid, Spain

increases at each site. As a consequence, the average magnitude of the transverse component S_t increases. Moreover, S_t becomes more widely distributed. A discrepancy exists, however, between the results of the Mössbauer spectra and the magnetic studies. An explanation can be found by considering the Rosencwaig canting model.[7] Scharner et al.[6] proposed order−disorder transitions for $x = 1.2$ and 1.57, but they did not suggest the possibility of canting in both positions.

The aim of the present work is to establish by means of neutron diffraction studies the behaviour of the phases, where $x = 1.28$ and 1.50, that are obtained by slowly cooling (SC) and rapid quenching (Q). The Rietveld refinement was used to solve the problem of the cation ordering in these phases, and additional magnetic measurements (ac and dc magnetic susceptibility and magnetisation curves) were performed to study the simultaneous substitution with nonmagnetic atoms in this series $Li_{0.5+0.5x}Fe_{2.5-1.5x}Ti_xO_4$.

Results and Discussion

Structural Features

Structural characterization at room temperature of the lithium ferrites with compositions $x = 1.28$ and 1.50 formed by slow cooling (SC) was carried out by neutron diffraction. The reflections were characteristic of a spinel structure in which some additional superstructural lines appear, and all these reflections were indexed satisfactorily on the basis of a cubic unit cell (Figure 1). Therefore, the SC samples exhibited cation ordering on the octahedral sites, resulting in a superstructure that could be refined in the $P4_332$ space group. We found, however, that a slight improvement in the fit was achieved by using a multiphase refinement using both the ordered ($P4_332$) and disordered ($Fd3m$) structures.[15,16] Rietveld analysis indicated that these samples are comprised of 94.9% superstructure (or ordered structure) and 5.1% disordered structure (for $x = 1.28$), and 82.3% superstructural component and 17.7% disordered component (for $x = 1.50$). Crystallographic data for both compounds obtained by Rietveld refinements are reported in Table 1 and the R-factors indicate a reliable structural model. The atomic coordinates are given in Table 2 and the most representative bond lengths are given in Table 3. These results suggest that the ordered structures have not been isolated as single phases under the present experimental conditions, although they are clearly in the majority, and this fact will certainly influence the magnetic behaviour of the materials.

At higher temperatures (1073 K for $x = 1.28$ and 973 K for $x = 1.50$), all the Bragg reflections were indexed on the basis of a cubic symmetry and the patterns were refined in the space group $Fd3m$. A good agreement between the calculated and observed patterns is shown in Figure 1. Therefore, the SC samples must undergo an order−disorder phase transition from the space group $P4_332$ to the space group $Fd3m$. Moreover, the neutron-diffraction pattern at 1073 K for $x = 1.50$ revealed the presence of an impurity,

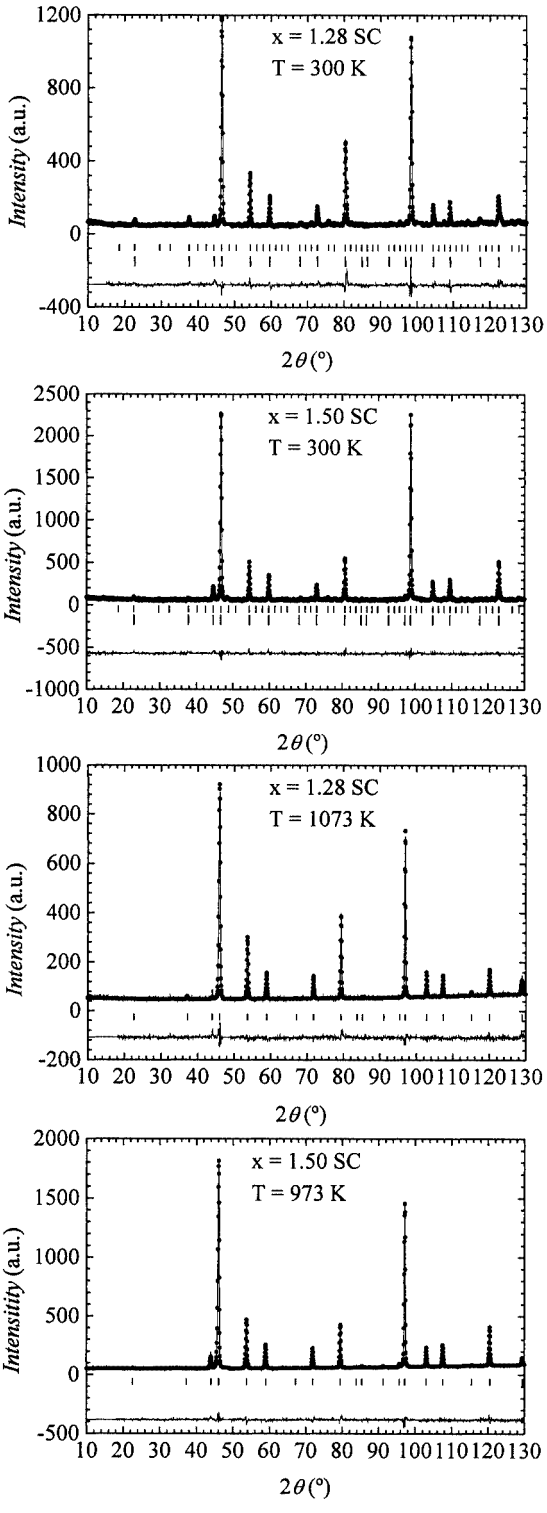

Figure 1. Observed, calculated and difference ND patterns of the slowly cooled (SC) samples at room temperature [peak positions of space group $P4_332$ (upper vertical marks) and $Fd3m$ (lower vertical marks) are indicated just below the patterns], and at different temperatures (space group $Fd3m$)

α-Fe_2O_3, whose amount increases with temperature, which suggests a decomposition process occurs for this spinel (pattern not shown). The most characteristic parameters obtained after the refinement are listed in Table 4 and a selec-

Table 1. Lattice parameters, *a*, and *R*-factors for $Li_{0.5+0.5x}Fe_{2.5-1.5x}Ti_xO_4$ (slow cooling) obtained by neutron refinement at room temperature

	x = 1.28 (ordered)		x = 1.50 (ordered)	
a [Å]	8.3725(4)	8.3701(9)	8.3549(2)	8.3689(8)
Space group	$P4_332$	*Fd3m*	$P4_332$	*Fd3m*
Z	8		8	
R_B [%]	5.78	7.64	4.49	8.56
R_P [%]	6.96		6.68	
R_{WP} [%]	9.47		8.74	
%	94.9	5.1	82.3	17.7

Table 2. Structural parameters obtained from the Rietveld refinement of neutron powder-diffraction patterns of $Li_{0.5+0.5x}Fe_{2.5-1.5x}Ti_xO_4$ (slow cooling) at room temperature (N = occupation)

x = 1.28				
$P4_332$ (ordered)			*Fd3m* (at random)	
8*c*			8*a*	
$x = y = z$		−0.0026(7)	$x = y = z$	⅛
N (Li / Fe)		0.68 / 0.32	N (Li / Fe)	0.61 / 0.39
4*b*			16*d*	
$x = y = z$		⅝	$x = y = z$	½
N (Li / Fe)		0.46 / 0.04	N (Li /Fe / Ti)	0.53 / 0.19 / 1.28
	x	⅛	32*e*	
12*d*	y	0.3877(5)	$x = y = z$	0.2583(6)
	z	0.8623(4)	N (O)	1/6
N (Fe / Ti)		0.22 / 1.28		
8*c*				
$x = y = z$		0.3919(1)		
N (O1)		⅓		
	x	0.1077(3)		
24*e*	y	0.1096(4)		
	z	0.3741(1)		
N (O2)		1		
x = 1.50				
$P4_332$ (ordered)			*Fd3m* (at random)	
8*c*			8*a*	
$x = y = z$		−0.0002(4)	$x = y = z$	⅛
N (Li / Fe)		0.77 / 0.23	N (Li / Fe)	0.79 / 0.21
4*b*			16*d*	
$x = y = z$		⅝	$x = y = z$	½
N (Li / Fe)		0.48 / 0.02	N (Li / Fe / Ti)	0.46 / 0.04 / 1.50
	x	⅛	32*e*	
12*d*	y	0.3629(6)	$x = y = z$	0.2763(4)
	z	0.8871(2)	N (O)	1/6
N (Ti)		1.50		
8*c*				
$x = y = z$		0.3861(8)		
N (O1)		⅓		
	x	0.1093(1)		
24*e*	y	0.1221(4)		
	z	0.3874(6)		
N (O2)		1		

Table 3. Selected bond lengths [Å] for $Li_{0.5+0.5x}Fe_{2.5-1.5x}Ti_xO_4$ obtained by SC.

x = 1.28			
$P4_332$ (ordered)		*Fd3m*(at random)	
d M(8*c*)−O1	1.944(9)	d M(8*a*)−O	1.930(7)(x4)
d M(8*c*)−O2	1.980(1)(× 3)	mean Shannon	1.931(1)
average d M(8*c*)−O	1.971(2)	d M(16*d*)−O	2.024(1)(× 6)
mean Shannon	1.938(1)	mean Shannon	2.050(2)
d M(4*b*)−O2	2.034(7)(× 6)		
mean Shannon	2.150(8)		
d M(12*d*)−O1	1.956(4)(× 2)		
d M(12*d*)−O2	2.049(3)(× 2)		
	2.067(7)(× 2)		
average d M(12*d*)−O	2.024(5)		
mean Shannon	2.316(3)		
x = 1.50			
$P4_332$ (ordered)		*Fd3m* (at random)	
d M(8*c*)−O1	1.946(9)	d M(8*a*)−O	2.271(7)(× 4)
d M(8*c*)−O2	1.972(2)(× 3)	mean Shannon	1.949(2)
average d M(8*c*)−O	1.965(8)	d M(16*d*)−O	1.864(6)(× 6)
mean Shannon	1.947(2)	mean Shannon	2.041(4)
d M(4*b*)−O2	2.068(5)(× 6)		
mean Shannon	2.155(4)		
d M(12*d*)−O1	2.089(1)(× 2)		
d M(12*d*)−O2	1.874(2)(× 2)		
	1.996(9)(× 2)		
average d M(12*d*)−O	1.986(7)		
mean Shannon	2.307(5)		

Table 4. Crystallographic data and structural parameters obtained from the Rietveld refinement of neutron powder-diffraction pattern of $Li_{1.14}Fe_{0.58}Ti_{1.28}O_4$ (SC) at 1073 K and $Li_{1.25}Fe_{0.25}Ti_{1.5}O_4$ (SC) at 973 K.

	x = 1.28	x = 1.50
a (Å)	8.4508(3)	8.4521(3)
Space group	*Fd3m*	*Fd3m*
Z	8	8
R_B (%)	4.81	4.68
R_P (%)	5.75	8.03
R_{WP} (%)	7.41	12.0
8*a*		
$x = y = z$	1/8	1/8
N[a] (Li/Fe)	0.67/0.33	0.86/0.14
16*d*		
$x = y = z$	1/2	1/2
N[a] (Li/Fe/Ti)	0.47/0.25 /1.28	0.39/0.11/1.50
32*e*		
$x = y = z$	0.2614(5)	0.2626(5)
N[a] (O)	1/6	1/6

[a] N = occupation.

tion of the most important interatomic distances are included in Table 5. On the other hand, for the samples obtained by quenching (Q), all the reflections can be indexed using the extinction laws of the space group *Fd3m*.[17,18] The resulting fits are shown in Figure 2 at 2 K (Figure 2, a) and 300 K (Figure 2, b). A summary of the structural parameters obtained in these refinements is given in Table 6 and 7.

The structure of SC samples were first reported by Blasse,[5] who described them as cation-ordered for x = 1.20 and x = 1.50. The 1:3 order on the octahedral sublattice is given by the lithium (4*b*) and titanium ions (12*d*), although the titanium sublattice contains some iron ions. Nevertheless, the Rietveld refinement of the neutron-diffraction data for our samples $(Li_{0.5x}Fe_{1-0.5x})_T(Li_{0.5}Fe_{1.5-x}Ti_x)_OO_4$ ob-

Table 5. Bond lengths [Å] for the samples $Li_{1.14}Fe_{0.58}Ti_{1.28}O_4$ (SC) at 1073 K and $Li_{1.25}Fe_{0.25}Ti_{1.5}O_4$ (SC) at 973 K.

d (M−O)	$x = 1.28$	$x = 1.50$
M(8*a*)−O	2.002(3) (× 4)	2.015(3) (× 4)
mean Shannon	1.937(2)	1.956(1)
M(16*d*)−O	2.025(2) (× 6)	2.011(9) (× 6)
mean Shannon	2.046(4)	2.037(4)

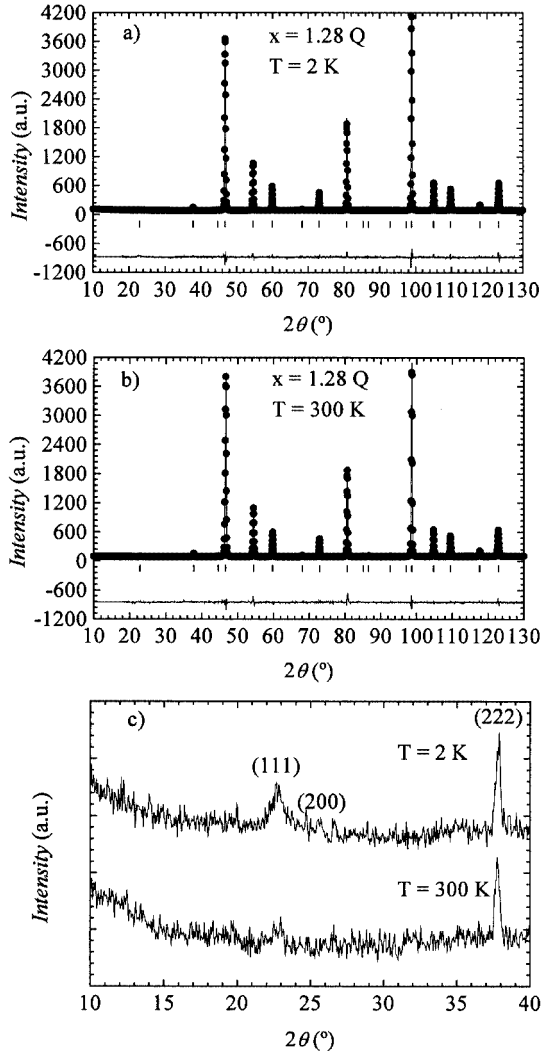

Figure 2. Neutron powder-diffraction pattern of the quenched (Q) compound with $x = 1.28$ at 2 K (a) and 300 K (b). Solid lines are the calculated profiles and dots are the experimental points. The difference profile is also shown. c) A comparison of the low-angle neutron diffraction patterns is shown at 2 and 300 K

tained by SC show that the cation distribution is slightly different from that suggested by Blasse in that the octahedral (4*b*) sites are occupied by Li^+/Fe^{3+} cations and the 12*d* sites are occupied by Fe^{3+}/Ti^{4+} cations. These samples show a cation-ordered superstructure with a minority disordered phase that also has been obtained for $Li_{0.5}Fe_{2.5-x}Cr_xO_4$.[16] The ordered form is close to an inverse spinel (space group $P4_332$) in which the 12*d* sites are

Table 6. Lattice parameter, *a*, *R*-factors and structural parameters for quenched (Q) $Li_{1.14}Fe_{0.58}Ti_{1.28}O_4$ at 2 K and at room temperature.

	$T = 2$ K	$T = 300$ K
a (Å)	8.3437(9)	8.3564(3)
Space group	*Fd*3*m*	*Fd*3*m*
Z	8	8
R_B (%)	3.43	3.34
R_P (%)	6.58	5.40
R_{WP} (%)	8.46	7.18
8*a*		
$x = y = z$	1/8	1/8
N[a] (Li/Fe)	0.65/0.35	0.66/0.34
16*d*		
$x = y = z$	1/2	1/2
N[a] (Li/Fe/Ti)	0.49/0.23 /1.28	0.48/0.24/1.28
32*e*		
$x = y = z$	0.2602(4)	0.2603(3)
N[a] (O)	1/6	1/6

[a] N = occupation.

Table 7. Bond lengths [Å] for $Li_{1.14}Fe_{0.58}Ti_{1.28}O_4$ Q at 2 K and at room temperature.

d (M−O)	$T = 2$ K	$T = 300$ K
M(8*a*)−O	1.955(1) (× 4)	1.958(7) (× 4)
mean Shannon	1.934(5)	1.936(2)
M(16*d*)−O	2.003(1) (× 6)	2.006(5) (× 6)
mean Shannon	2.047(5)	2.047(1)

occupied by iron and titanium ions giving rise to different M−O distances (Table 3, Table 5 and Table 7), whereas the Li^+/Fe^{3+} ions occupy the centre of regular octahedral 4*b* sites. The disordered form is an inverse spinel (space group *Fd*3*m*) in which the $Li^+/Fe^{3+}/Ti^{4+}$ atoms are distributed randomly over the regular octahedral sites, and the tetrahedral ones are occupied by Li^+/Fe^{3+} ions. Figure 3 illustrates these features in a fragment of the ordered (Figure 3, a) and disordered (Figure 3, b) structures. Finally, the values obtained in the refinement of the unit cell parameters for all samples reflect the abovementioned changes in the cationic site distribution resulting from an intracrystalline order−disorder process.[6]

Magnetic Behaviour

Figure 4 shows the dependence of the dc magnetic susceptibility of the title samples with temperature $\chi(T)$ in the range between 2 and 300 K measured at a field of 0.5 kOe. The $\chi(T)$ variation for the composition $x = 1.28$ (SC and Q) shows broad maxima at about 20 K and 17 K, respectively. The dc magnetic susceptibility decreases with temperature for the sample $x = 1.50$ (SC and Q). We observed that the magnetic susceptibility is remarkably smaller for the disordered samples than for the ordered ones, and this fact is consistent with a decrease of ordering. No Curie−Weiss behaviour was observed over the whole tem-

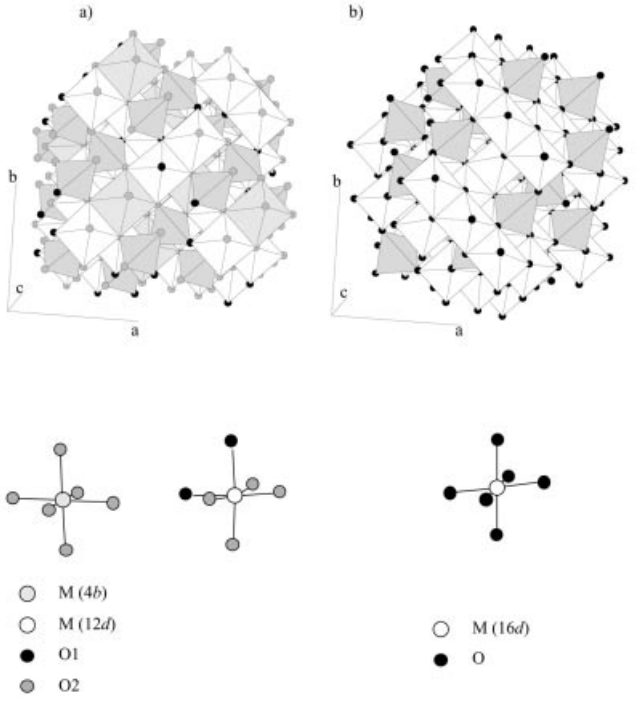

Figure 3. The structure of the $Li_{0.5+0.5x}Fe_{2.5-1.5x}Ti_xO_4$ spinels: a) ordered form (space group $P4_332$); b) disordered form (space group $Fd3m$)

perature range measured from the dc reciprocal susceptibility. The absence of a linear behaviour towards high temperature suggests that a ferrimagnetic transition is expected for a Curie temperature $T_C > 300$ K and, for example, these results are depicted in Figure 4 (part e) for the Q sample with $x = 1.28$ at $H = 1.5$ kOe.

Magnetisation measurements were performed in the temperature range $5 \leq T \leq 375$ K and some results are shown in Figure 5. We see that the magnetization increases with increasing applied field for each composition. In the present range of the magnetizing field, the magnetization does not show a saturation and it decreases slightly with increasing titanium content, in agreement with Néel's theorem of ferrimagnetism.[19] The individual magnetization in the A (tetrahedral) and B (octahedral) sites, M_A and M_B, of the two sublattices cannot be observed, but the net magnetization has been measured instead. Because the two magnetizations are oppositely directed, then $M = M_A - M_B$. The variation of magnetic moment with titanium content can be explained by assuming that, as the concentration of titanium ion increases, the relative number of Fe^{3+} ions decreases on both the A and B sites, but more on the B sites than on the A sites. This distribution is expected to disminish the A−B interactions, which in spinels, according to Néel's molecular field model, are stronger than A−A or B−B ones. Obviously, Ti^{4+} does not participate in any exchange interactions, but disminishes those resulting from the $Fe_A^{3+}-O-Fe_B^{3+}$ unit and the net effect is a decrease in the overall magnetization. Considering the spin-only moment for Fe^{3+} of 5 μ_B, the saturation moments have been estimated as being 0.3 μ_B and 1.05 μ_B for $x = 1.28$ and $x = 1.50$, respectively, but the values obtained at the highest fields (see Figure 5) are smaller than those expected from a collinear model. On the other hand, when the temperature is lowered, the magnetization curves below T_C show a clear ferromagnetic component with increasing importance. Such behaviour is evidence for a disordered spin-state (SG-like state) induced by disorder and frustration because of competing ferro- and antiferromagnetic exchange interactions.

As an example of the general behaviour, Figure 6 shows, for $x = 1.28$ (Q), the variation of the ac susceptibility with temperature ranging between 1.8 and 350 K at a magnetic field of 0.215 Oe for frequencies changing from 0.1 to 10 kHz. The susceptibility increases with increasing temperature, exhibiting a cusp, and then a marked decay. The cusp temperature is ca. 14−15 K, which is consistent with that observed in the dc measurement shown in Figure 4b. The inset of Figure 6 reflects that the cusp shows frequency dependence; it shifts to higher temperatures with increasing frequency and this feature is characteristic of the spin-glass behaviour stated above.

The spin-glass state occurs because of a combination of "randomness" and "frustration" in spin ordering, caused by the randomly mixed state of the ferromagnetic (spin-parallel) and antiferromagnetic (spin-antiparallel) spin interactions.[20] To obtain the spin-glass state in spinel ferrites, it is usual to substitute Fe^{3+} ions by nonmagnetic ions, such as Li^+ and Ti^{4+}, which results in the dilution of magnetic interactions (randomness) and the competition of exchange interactions (frustration). In this sense, Figure 7 shows a simplified model of the spin-glass phenomenon in a spinel ferrite AB_2O_4, in which the nearest neighbours of interacting metal ions bridged via the O^{2-} anion are shown. A denotes a tetrahedral site cation and B an octahedral one. In spinel oxides, the magnetic ions interact with each other through super-exchange antiferromagnetic interactions for which $|J_{AB}| >> |J_{BB}| > |J_{AA}|$ (J being the average value of the spin interactions). Thus, J_{AB} renders the undiluted spinel ferrimagnetism, with all A-site moments oriented antiparallel to all B-site moments, with BB and AA bonds remaining unsatisfied (left-hand side of Figure 7). After dilution of Fe^{3+} ions in the B sites by Li^+ and Ti^{4+} ions substitution, the magnetic order is broken and the frustration of certain moments occurs for BB and AA bonds (right-hand side of Figure 7).

To take into account the magnetic contribution to the Bragg diffraction peaks, the thermal evolution of the NPD patterns was acquired in the temperature ranges between 2−300 K, for $x = 1.28$ (SC) and 1.28 (Q), and 2−112 K, for $x = 1.50$ (Q), with $\lambda = 2.522$ Å and are shown in Figure 8a, 8b and 8c, respectively. Rietveld refinements in those temperature ranges were attempted, with and without a magnetic contribution, but the variation in intensity of the inner Bragg peaks — namely (111), (220), (311), (222), etc. — with the decrease in temperature was scarcely apparent, and this fact seems to indicate the absence of any magnetic long-range ordering (LRO) in these samples.[21]

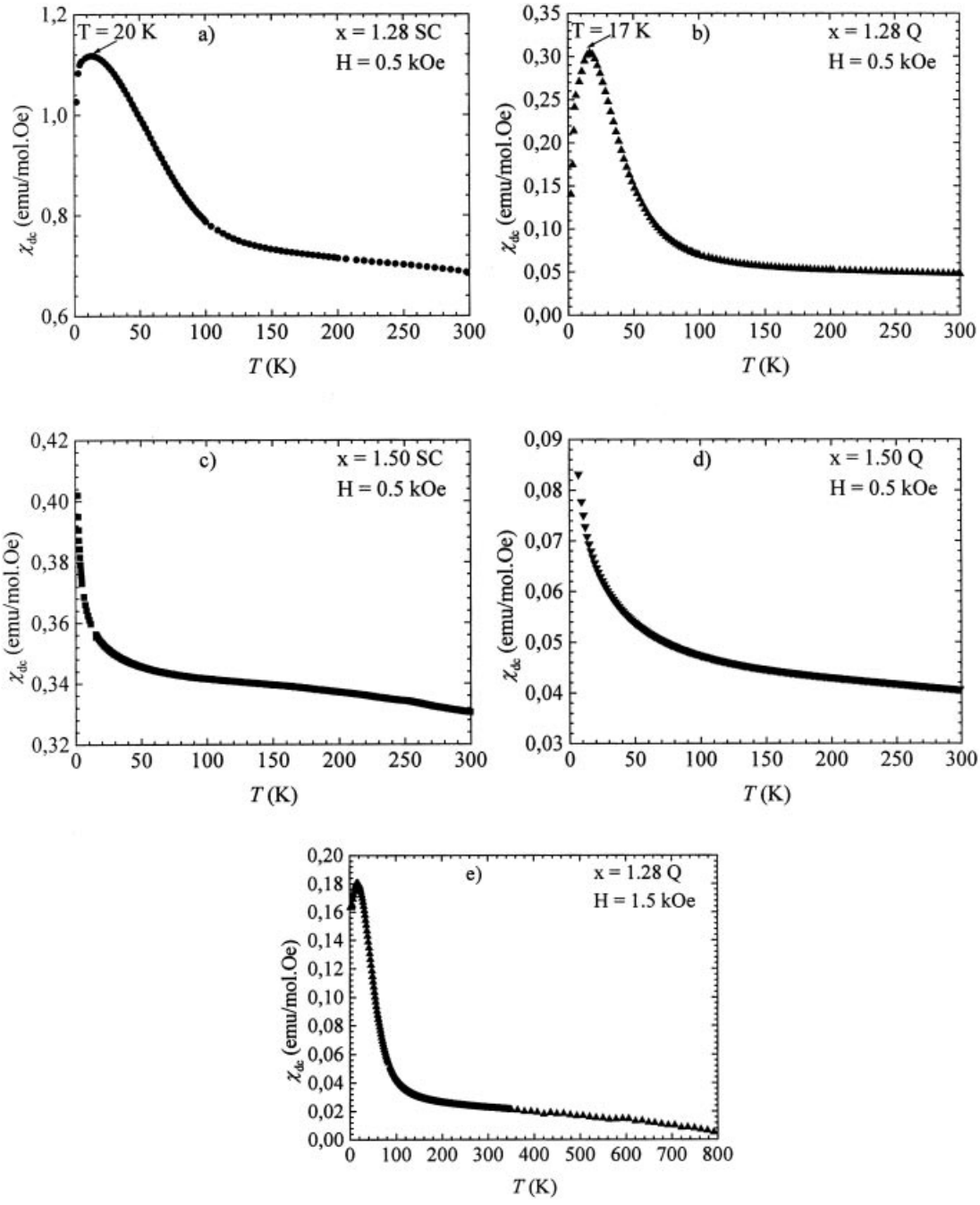

Figure 4. Variation of the dc magnetic susceptibility with temperature for $Li_{0.5+0.5x}Fe_{2.5-1.5x}Ti_xO_4$: $x = 1.28$ (SC and Q) and $x = 1.50$ (SC and Q). Applied field: 0.5kOe (a−d) and 1.5 kOe (e)

On the other hand, Figure 2 (part c) shows the variation of the (111) peak at 2 and 300 K for the sample $x = 1.28$ (Q), in which we see a slight increase in intensity at the lower temperature that seems to indicate a magnetic contribution. Moreover, it is noticeable that there is a considerable broadening of the (111) reflection, which suggests the presence of magnetic spin clusters.[22] Such a variation was not observed for our sample $x = 1.50$, from which the experimental data indicate a characteristic spin-glass behaviour.

Conclusions

Neutron-diffraction experiments were performed on lithium titanium ferrite $Li_{0.5+0.5x}Fe_{2.5-1.5x}Ti_xO_4$ ($x = 1.28$ and 1.50). The data show that the samples obtained by SC are ordered spinels of 1:3 type at octahedral sites, where Li^+ ions occupy octahedral (4*b*) and tetrahedral (8*c*) sites, Fe^{3+} cations are distributed over the octahedral (4*b* and 12*d*) and tetrahedral (8*c*) sites, and Ti^{4+} ions are exclusively located on octahedral (12*d*) sites. When the samples were quenched,

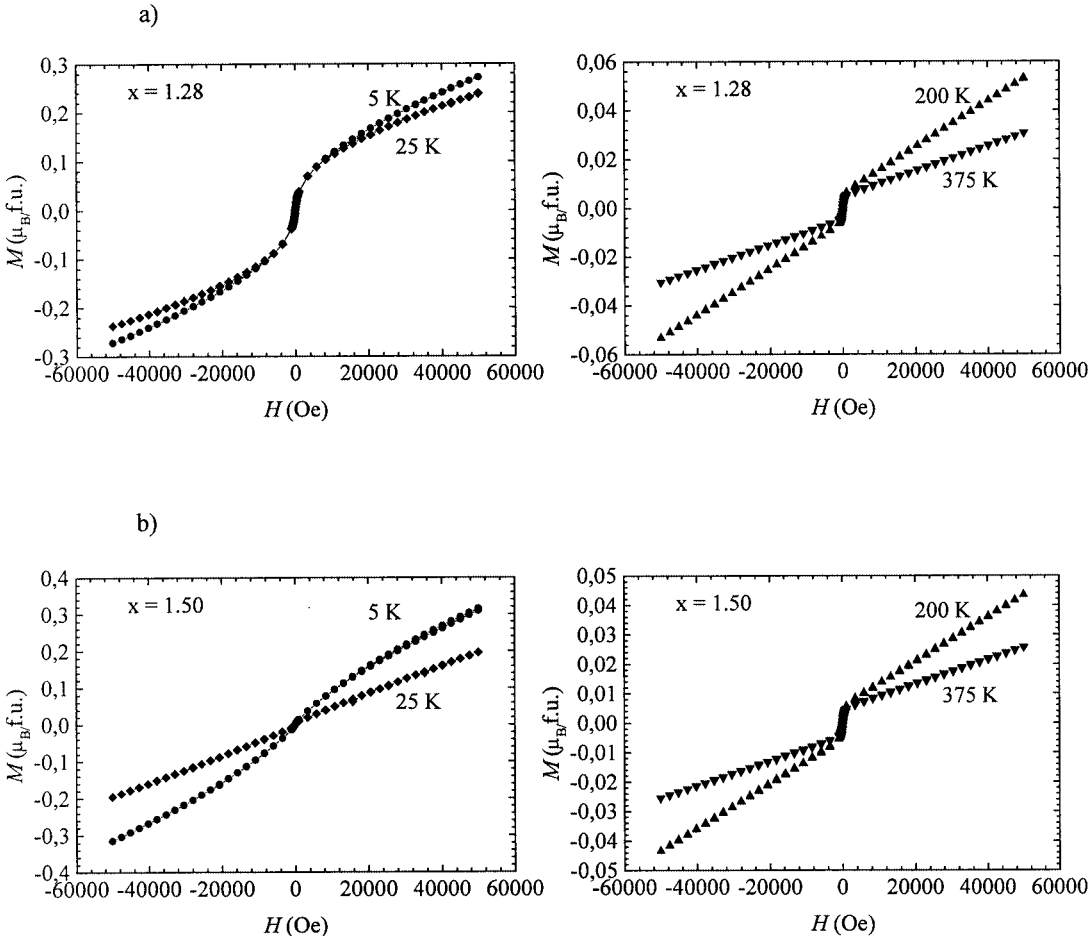

Figure 5. Isothermal magnetization vs. magnetic field at different temperatures for the samples obtained by quenching: a) $x = 1.28$; b) $x = 1.50$

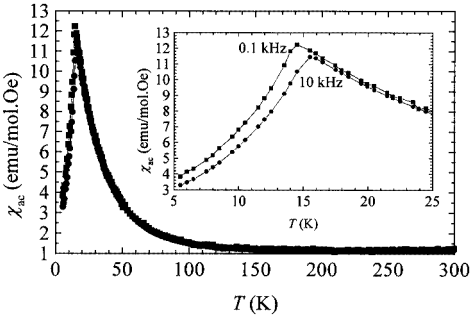

Figure 6. Real part of the ac magnetic susceptibility as a function of temperature from 1.8 to 350 K for $x = 1.28$ (Q) at $\nu = 0.1$ and 10 kHz, $H = 0.215$ Oe. Inset: temperature interval 5−25 K

the 1:3 ordering was destroyed and a change of symmetry occurred from $P4_332$ to $Fd3m$, so that the tetrahedral sites become occupied at random by Li^+/Fe^{3+} ions and the octahedral sites by $Li^+/Fe^{3+}/Ti^{4+}$ ions. Magnetic and neutron-diffraction measurements carried out on these samples confirm a spin-glass behaviour that is attributed to dilution of Fe^{3+} ions in the B sites by the substitution effect of Li^+ and Ti^{4+} ions. Therefore, magnetic order is broken and the

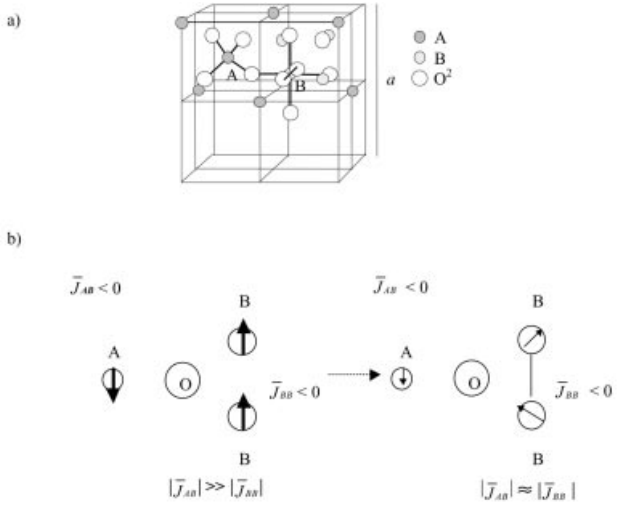

Figure 7. (a) Two octants in the unit cell of the spinel structure with lattice parameter a. The O^{2-} anions form a cubic close-packed structure, with A ions occupying the tetrahedral sites (A site), and B ions occupying the octahedral sites (B site). (b) Model of the spin-glass phenomenon in spinel ferrite. The nearest neighbours of the metal ions bridged via the O^{2-} anion in the spinel ferrite are shown: A (tetrahedral site cation), B (octahedral site cation). Arrows correspond to the spin of Fe ion

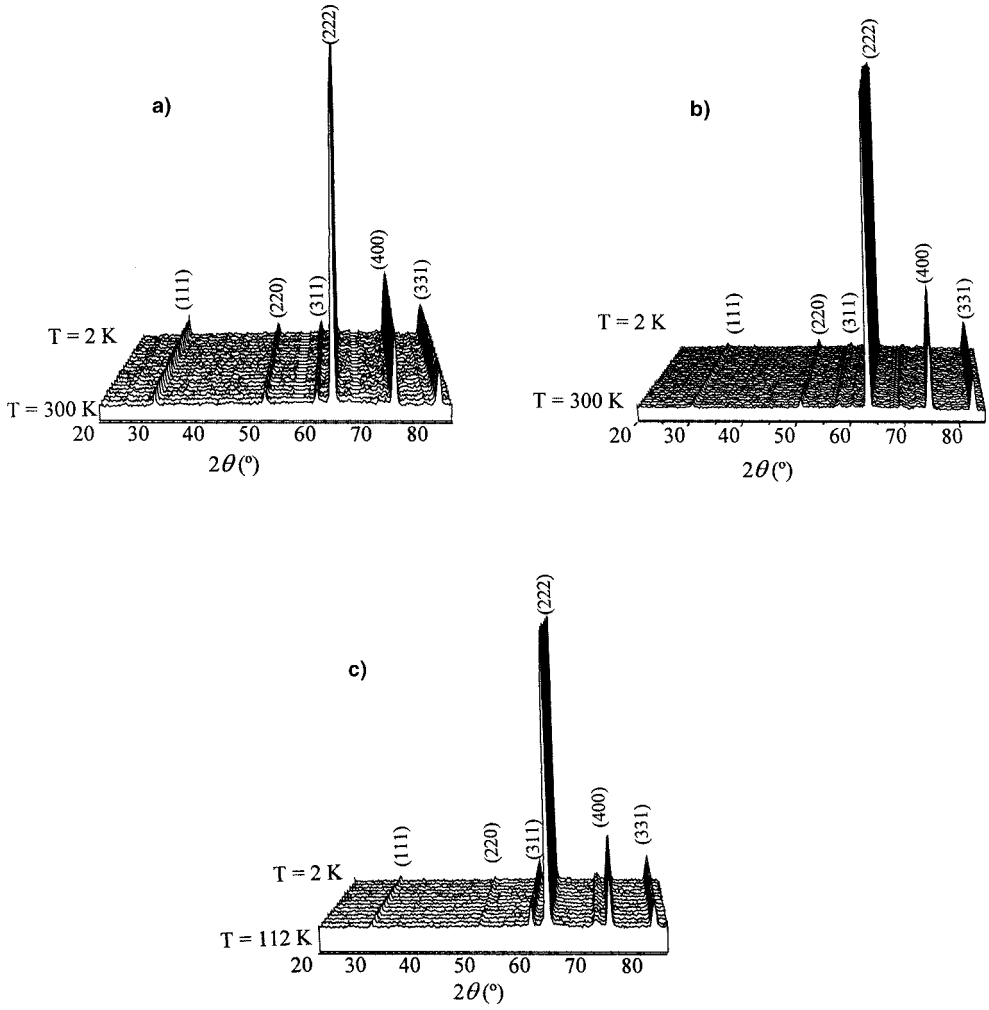

Figure 8. Thermal evolution of NDP collected at a wavelength λ = 2.522 Å in the following temperature ranges: a) 2−300 K (x = 1.28, SC), b) 2−300 K (x = 1.28, Q), c) 2−112 K (x = 1.50, Q)

frustration of certain moments occurs for BB and AA interactions.

Experimental Section

Polycrystalline samples of $Li_{0.5+0.5x}Fe_{2.5-1.5x}Ti_xO_4$ (where x = 1.28 and 1.50) were prepared by the "liquid mix" technique[23] from powdered mixtures of Li_2CO_3, Fe_2O_3 and TiO_2 (all reactants were supplied by Merck, Germany) in stoichiometric ratios. The samples were obtained by two methods: slow cooling (SC, at 1073 K for a day) or rapid quenching (Q) from temperatures above 1073 K for 12 h (x = 1.28) and 973 K for 12 h (x = 1.50) to room temperature.

Neutron powder-diffraction data were obtained at different temperatures for the samples x = 1.28 (ordered and disordered phases) and x = 1.50 (ordered phase) on the D1A high-resolution powder diffractometer (λ = 1.9110 Å) at the Institute Laue-Langevin (Grenoble, France). The multidetector D1B powder diffractometer with a wavelength of 2.522 Å was used to obtain the thermal patterns in the temperature ranges 2−300 K for x = 1.28 (ordered and disordered phases) and 2−112 K for x = 1.50 (disordered phase). Diffraction patterns were analysed by the Rietveld[24] method and the Fullprof programme.[25]

The magnetic-susceptibility measurements were performed using a commercial superconducting quantum-interference-device magnetometer, Quantum Design Magnetic Properties Measurement System 5S, on powder samples in a temperature range from 1.8 to 300 K under an applied magnetic field of 0.215 Oe. The magnetic field isothermal variations up to 60 kOe were obtained with the aid of a Quantum Design Physical Properties Magnetic System, which allowed the experimental setting of highly homogeneous magnetic fields at specific temperatures.

Acknowledgments

We are indebted to the CYCIT (MAT, 2002−01288) for financial support. We acknowledge the ILL and CR1G−D1B for collecting ND data. M.A.A. is grateful to the Comunidad de Madrid for a Postdoctoral Fellowship and A.S.B. thanks the Ministry of Education, Sports and Culture of Spain for financial support under a Postdoctoral Research Fellowship.

[1] M. Guillot, *Magnetic Properties of Ferrites* (Ed.: K. H. J. Buschow), *Electronic and Magnetic Properties of Metals and Ceramics*, Wiley-VCH, Weinheim, Germany, **1994**.
[2] P. B. Braun, *Nature* **1952**, *27*, 1123.
[3] S. J. Marin, M. O′Keeffe, D. E. Partin, *J. Solid State Chem.* **1994**, *113*, 413−419.
[4] J. L. Dormann, A. Tomas, M. Noguès, *Phys. Status Solidi* **1983**, *77*, 611−618.
[5] G. Blasse, *Philips Res. Repts. Suppl.* **1964**, *3*, 96−102.
[6] S. Scharner, W. Weppner, P. Schmid-Beurmann, *J. Solid State Chem.* **1997**, *134*, 170−181.
[7] J. L. Dormann, M. El Harfaoui, M. Nogues, J. Jové, *J. Phys. C* **1987**, *20*, L161−L166.
[8] J. L. Dormann, M. Noguès, *J. Phys.: Condens. Matter.* **1990**, *2*, 1223−1237.
[9] M. Seqqat, J. L. Dormann, M. Nogues, J. Jové, G. Nicoara, *Hyp. Inter.* **1994**, *94*, 2017−2021.
[10] G. O. White, C. E. Patton, *J. Magn. Magn. Mater.* **1978**, *9*, 299−317.
[11] M. El Harfaoui, J. L. Dormann, M. Noguès, G. Villers, V. Gaignaert, F. Bouree-Vigneron, *J. Physique Colloq.* **1988**, C8, *49*, 1147−1148.
[12] M. Noguès, M. Seqqat, F. Bouree-Vigneron, J. L. Dormann, G. Nicoara, *J. Magn. Magn. Mater.* **1992**, *104−107*, 1643−1644.
[13] M. Godinho, A. Carvalho, M. Noguès, J. L. Dormann, M. Seqqat, *J. Magn. Magn. Mater.* **1994**, *133*, 457−459.
[14] A. Belayachi, J. L. Dormann, M. Noguès, *J. Phys.: Condens. Matter.* **1998**, *10*, 1599−1619.
[15] W. Branford, M. A. Green, D. A. Neumann, *Chem. Mater.* **2002**, *14*, 1649−1656.
[16] L. Fernández-Barquín, M. V. Kuznetsov, Y. G. Morozov, Q. A. Pankhurst, I. P. Parkin, *Inter. J. Inorg. Mater.* **1999**, *1*, 311−316.
[17] M. A. Arillo, M. L. López, E. Perez-Cappe, C. Pico, M. L. Veiga, *Solid St. Ionics* **1998**, *107*, 307−312.
[18] M. A. Arillo, M. L. López, C. Pico, M. L. Veiga, J. Campo, J. L. Martínez, A. Santrich-Badal, *Phys. Rev. B*, in press.
[19] K. Standly, *Oxide Magnetic Materials*, Clarendon, Oxford, **1972**.
[20] S. F. Edwards, P. W. Anderson, *J. Phys. F: Met. Phys.* **1975**, *5*, 965−974.
[21] S. M. Yunus, H.-S. Shim, C.-H. Lee, M. A. Asgar, F. U. Hamed, A. K. M. Zakaria, *J. Magn. Magn. Mater.* **2001**, *232*, 121−132.
[22] S. M. Yunus, J. A. Fernández-Baca, M. A. Asgar, F. U. Ahmed, M. A. Hakim, *Physica B* **1999**, *262*, 112−124.
[23] M. Pechini, *U. S. Patent*, **1996**, 3 231/328.
[24] H. M. Rietveld, *J. Appl. Cryst.* **1969**, *2*, 65−71.
[25] J. Rodríguez Carvajal, FULLPROF, XV Congress of International Union of Crystallography, Toulouse **1990**, p. 127 (Revised version, **1994**).

Received December 20, 2002

